Journal of Cleaner Production 319 (2021) 128605

Contents lists available at ScienceDirect

Journal of Cleaner Production

journal homepage: www.elsevier.com/locate/jclepro

Improving efficiency and feasibility of subcritical water debromination of printed circuit boards E-waste via potassium carbonate adding

Gerard Gandon-Ros [a,b,*], Aurora Soler [a,b], Ignacio Aracil [a,b], María Francisca Gómez-Rico [a,b], Juan A. Conesa [a,b]

[a] Institute of Chemical Process Engineering, University of Alicante, P.O. Box 99, E-03080, Alicante, Spain
[b] Department of Chemical Engineering, University of Alicante, P.O. Box 99, E-03080, Alicante, Spain

ARTICLE INFO

Handling editor: Cecilia Maria Villas Bôas de Almeida

Keywords:
Hydrothermal process
Debromination efficiency
Printed circuit boards
E-Waste
Alkaline additive
Potassium carbonate

ABSTRACT

Waste printed circuit boards (WCBs) were debrominated under hydrothermal treatment, using potassium carbonate as an alkaline additive to improve debromination efficiency (DE). Two different high-pressure reactors were used: a 1-L stirred reactor, where the evolution of the DE was followed over time at a low CO_3^{2-}/Br^- ratio (1:25), and an elementary 0.1-L non-stirred reactor, used to find the optimal parameters and to simplify the hydrothermal debromination (HTD) process. Considering both reactors, experiments were conducted changing the temperature (200 °C, 225 °C, 250 °C, 275 °C), and also the CO_3^{2-}/Br^- anionic ratio (1:50, 1:25, 1:10, 1:5, 1:2.5, 1:1, 2:1, 4:1) and the solid/liquid ratio (1:10, 1:5, 1:2) in the case of the 0.1-L reactor. No metallic catalyst was required.

A maximum DE of about 98.9 wt % was reached in the agitated vessel at 275 °C after 4 h, with an additive/bromine ratio of 1:25. Similar DE (99.6 wt %) was also achieved in the non-stirred reactor at only 225 °C and after 2 h, using an additive/bromine ratio of 4:1 and a solid/liquid ratio of only 1:2. Concerning the solid phase behaviour during debromination, only 5 % of the net calorific value (NCV) was lost after a complete HTD treatment of WCB.

1. Introduction

Over the last years, waste electrical and electronic equipment (WEEE) has increased significantly worldwide, due to notable technological innovations and society's irresponsible levels of consumption. In 2016, some 44.7 million metric tons (Mt) of WEEE were generated worldwide (Baldé et al., 2017). A total of 80% was incinerated or accumulated in landfills, which entail a significant risk to the environment (Owens et al., 2007) and human health (Leung et al., 2008) if no appropriate control measurements are taken. In Europe, the latest WEEE Directive (European Commission and Comisión Europea, 2012) aims at preventing the generation of WEEE and promotes the reuse, recycling and other forms of recovery of WEEE.

The recycling of WEEE involves the recovery of raw materials such as metals and plastics, and the responsible elimination of environmentally dangerous substances such as brominated flame retardants (BFRs) and heavy metals (Buekens and Yang, 2014).

Printed circuit boards (PCBs) represent approximately 6% of the total weight of WEEE (Das et al., 2009) and are one of the most complex constituents of these types of wastes. Typically, PCBs contain 30% of metals such as copper, tin, lead, iron, nickel and precious metals (Goosey and Kellner, 2002, 2003), while the rest is composed by thermosetting resins, reinforcing materials, BFRs and other additives (Guo et al., 2009). BFRs represent between 5 and 15 % of the total weight of WCBs (Chien et al., 2000). The main BFRs used are polybrominated biphenyls (PBB), hexabromocyclododecanes (HBCDD), polybrominated diphenyl ethers (PBDE) and tetrabromobisphenol A (TBBPA), the latter BFR being one of the most extensively used worldwide (Soler et al., 2017).

The recycling process of WCBs is based on recovering metals as the most valuable components. However, their recycling can generate emissions of polychlorinated dioxins and furans (PCDD/Fs) (Nie et al., 2012; Pitea et al., 2008). Therefore, this waste must be split into two fractions (metallic and non-metallic) to separate their recycling. The non-metallic fraction has traditionally been considered a low-value product and heat-treated in an uncontrolled way (Kim et al., 2015) or simply landfilled (Ning et al., 2017). During thermal treatments, toxic

* Corresponding author. Institute of Chemical Process Engineering, University of Alicante, P.O. Box 99, E-03080, Alicante, Spain.
E-mail address: gerard.gandon@ua.es (G. Gandon-Ros).

https://doi.org/10.1016/j.jclepro.2021.128605
Received 23 September 2020; Received in revised form 7 July 2021; Accepted 9 August 2021
Available online 13 August 2021

compounds such as polybrominated dibenzo-p-dioxins/furans (PBDD/Fs) can be emitted (Altarawneh and Dlugogorski, 2015; Sakai et al., 2001) while landfilling can lead to the soil and groundwater being contaminated by the leachate, which contains brominated toxic compounds (Zhou et al., 2013) as well as heavy metals (Akcil et al., 2015; Hadi et al., 2015); it can also pollute the atmosphere through the evaporation of hazardous substances (Guo et al., 2012). Controlled thermal treatments could be useful to obtain fuels or recover valuable materials, but brominated toxic compounds can be still emitted.

The debromination treatment of WCBs using subcritical or supercritical water prior to thermal treatments such as pyrolysis or combustion has become a promising technique today because excellent debromination efficiencies can be obtained and then brominated toxic emissions could be reduced. Wang and Zhang (2012) compared debromination efficiencies in various supercritical fluids (water, methanol, isopropanol and acetone) and achieved with water a debromination efficiency of 97.6 % from brominated flame retardant (BFR) and BFR-containing waste computer housing plastic at 400 °C in 60 min. Xing and Zhang (2013) removed 97.7% of the bromine present in WCBs with a S/L (solid/liquid) ratio equal to 1:4 g/mL at 400 °C for 2 h. Xiu et al. (2014) achieved the total removal of bromine from PCBs fraction at 350 °C in 60 min and solid/liquid ratio 1:9 g/mL. Soler et al. (2017) used lower temperatures (225–275 °C) and also observed a decrease in the emissions of brominated compounds during subsequent thermal treatment. Yin et al. (2011) compared subcritical and supercritical water conditions and the addition of different reagents. The addition of the dilute solutions of acetic acid or sodium hydroxide increased the debromination efficiency compared to using only water.

The main objective of this work was to optimise the operation parameters for WCBs debromination treatment in order to improve HTD feasibility for a possible future industrialization of this process. An almost complete debromination was achieved in a reasonable time by using a standard high-pressure reactor in subcritical conditions and by reducing as much as possible the temperature treatment (and therefore energy requirements) using water as solvent. K_2CO_3, which is a simple alkaline additive with a low price, was added for that purpose because of its recommendable behaviour with regard to improving the efficiency of PVC waste dechlorination, as demonstrated by Gandon-Ros et al. (2020).

Experiments were carried out changing the temperature, the CO_3^{2-}/Br^- anionic ratio and the solid/liquid ratio (g of PCB/mL of K_2CO_3 dissolution), using two different high-pressure reactors: a 1-L stirred reactor where the evolution of the DE with time at low CO_3^{2-}/Br^- ratio was followed, and an elementary non-stirred reactor to find optimal parameters and to simplify the HTD process.

2. Materials and methods

2.1. Materials

In the present work, metal-free WCBs were employed. CISA (Circuitos Impresos S.A., Spain) supplied those circuit boards, which are a high-quality standard FR-4 epoxy fibreglass substrate. In a previous study, Soler et al. (2017) confirmed by Raman spectroscopy that these FR-4 WCBs contained TBBPA as BFR.

WCBs were cut into 20 mm × 40 mm pieces using pliers and were later crushed into small-sized particles between 0.84 mm × 0.84 mm and 4 mm × 4 mm using a cutting mill RETSCH SM200 (Haan, Germany). Elemental analysis (27.55 wt% C, 2.54 wt% H, 1.06 wt% N and 24.56 wt% O) was performed in a Thermo Finnigan Flash 1112 Series Elemental Analyzer. Ash content was 44.29 wt% measured at 550 °C, in accordance with the UNE-EN-14775:2009 (ECS, 2010). Bromine content was measured using the US EPA Methods 5050 (US EPA, 1994) and 9056A (US EPA, 2000) by oxygen combustion bomb-ion chromatography (Dionex DX-500), the average value being 4.05 wt%.

K_2CO_3 was reactive-quality grade with a minimum purity of 99 % and was supplied by Merck (Darmstadt, Germany).

2.2. Subcritical water debromination set-up

Debromination runs, using several dilute solutions of K_2CO_3 as subcritical fluid, were performed at different temperatures in high pressure batch reactors of 1-L volume (stirred) and 0.1-L volume (non-stirred). The stirred reactor (named "1 L-stirred" hereinafter) was a RS1000-SMH (Ilshin Autoclave, Korea) made of 304 stainless steel that offers working pressures up to 20 MPa and operating temperatures up to 350 °C. The non-stirred reactor ("0.1 L-non stirred") was a Baoshishan autoclave (Baoshishan, China) built with a 304 stainless steel shell and PTFE chamber able to resist acid and alkali for a maximum pressure of 3 MPa, a safe temperature of 220 °C and a heating/cooling gradient temperature under 5 °C min^{-1}. The parameters controlling the efficiency of the debromination process in both reactors were: a K_2CO_3 concentration of dilute solution, operating temperature, residence time and solid/liquid (S/L) ratio.

2.3. Experiments and conditions

In this study, a total of 33 debromination experiments were performed at 200, 225, 250 and 275 °C during 120–240 min, with a CO_3^{2-}/Br^- ratio (r) of 1:50, 1:25, 1:10, 1:5, 1:2.5, 1:1, 2:1, 4:1 and different S/L ratios equal to 1:10, 1:5, 1:2 and 1:1 g/mL, thus exceeding the previously established useful limit for the S/L ratio (Xing and Zhang, 2013). Table 1 shows the nomenclature and conditions used for each experiment. Some experiments were replicated in order to determine an experimental reproducibility with an experimental error below 9 %. Although both reactors were employed, the performance obtained for the 0.1 L-non stirred reactor was considered more appropriate due to its simplicity and pertinence regarding the search for the optimal parameters for WCB debromination, as shown in Table 1.

During the debromination runs in the 1 L-stirred reactor, liquid samples were collected every hour and the remaining liquid from the reaction chamber was also collected after 24 h in order to evaluate the evolution of the debromination process with time at different treatment temperatures of 225, 250 and 275 °C. These liquid samples were analysed for bromine by ion chromatography taking into account that the evolution of the DE with time for each condition was obtained from measured concentrations, properly corrected due to the reduction of mass solution over time inside the reaction chamber (Gandon-Ros et al., 2020). The analysis of reaction products as well as the determination of mechanisms and reaction kinetics were outside the scope of this work. They are pending for future research due to the large amount of information presented. Additionally, a smaller particle size was used in the experiment at 225 °C than in the experiments at 250 °C and 275 °C, being under 0.84 and under 4 mm respectively. The aim was to evaluate the relative importance of WCBs size before HTD. Every set temperature was attained under a heating rate of about 2.5 °C/min and the stirrer was rotating at 100 rpm in all runs to ensure that the temperature and the sample were properly homogeneous in the batch during the whole treatment.

Moreover, to obtain the optimal conditions for a suitable and efficient HTD process, which requires less input energy and maintenance, an easy-to-use 0.1 L-non stirred standard reactor was employed. For these experiments, a smaller particle size (under 0.84 mm) was used, the residence time was set to 2 h and the influence of temperature, solid/liquid ratio and additive concentration was investigated, taking care not to surpass the limit pressure inside the chamber. The pressure in the stirred reactor was the vapour pressure of the mix taking into account the temperature value. In order to perform this latter calculation, a reactor chamber of volume V was considered, which is directly related to the volume of added solid, as well as a mixture of liquid and gas phases generated at temperature T following equations (1) and (2):

Table 1
Experimental conditions assessed.

Experiment	T/°C	Time at set temperature (h)	Weight WCB (g)	Anionic CO_3^{2-}/Br^- ratio	Solid/Liquid ratio	Employed Reactor
225.0	225	0–4	100.0	1:25	1:5	1 L-stirred
250.0	250	0–4	100.0	1:25	1:5	1 L-stirred
275.0	275	0–4	100.0	1:25	1:5	1 L-stirred
200.1	200	2	5.0	1:25	1:5	0.1 L-non stir.
200.2	200	2	5.0	1:50	1:5	0.1 L-non stir
200.3	200	2	5.0	1:10	1:5	0.1 L-non stir
200.4	200	2	2.5	1:25	1:10	0.1 L-non stir
200.5	200	2	2.5	1:50	1:10	0.1 L-non stir
200.6	200	2	5.0	1:10	1:5	0.1 L-non stir
200.7	200	2	5.0	1:5	1:5	0.1 L-non stir
200.8	200	2	5.0	1:2.5	1:5	0.1 L-non stir
200.9	200	2	10.0	1:25	1:2.5	0.1 L-non stir
200.10	200	2	10.0	1:50	1:2.5	0.1 L-non stir
200.11	200	2	5.0	1:1	1:5	0.1 L-non stir
200.12	200	2	5.0	2:1	1:5	0.1 L-non stir
200.13	200	2	5.0	4:1	1:5	0.1 L-non stir
200.14	200	2	10.0	1:25	1:1	0.1 L-non stir
200.15	200	2	10.0	1:50	1:1	0.1 L-non stir
200.16	200	2	12.5	1:25	1:2	0.1 L-non stir
200.17	200	2	12.5	1:2.5	1:2	0.1 L-non stir
200.18	200	2	12.5	1:1	1:2	0.1 L-non stir
200.19	200	2	12.5	2:1	1:2	0.1 L-non stir
200.20	200	2	12.5	4:1	1:2	0.1 L-non stir
225.1	225	2	5.0	1:25	1:5	0.1 L-non stir
225.2	225	2	5.0	1:50	1:5	0.1 L-non stir
225.3	225	2	5.0	1:10	1:5	0.1 L-non stir
225.4	225	2	2.5	1:25	1:10	0.1 L-non stir
225.5	225	2	2.5	1:50	1:10	0.1 L-non stir
225.6	225	2	12.5	1:25	1:2	0.1 L-non stir
225.7	225	2	12.5	1:2.5	1:2	0.1 L-non stir
225.8	225	2	12.5	1:1	1:2	0.1 L-non stir
225.9	225	2	12.5	2:1	1:2	0.1 L-non stir
225.10	225	2	12.5	4:1	1:2	0.1 L-non stir

$$log_{10}P_v = A - \frac{B}{C+T} \quad (1)$$

where P_v is the water vapour pressure in mm Hg, T is the temperature in °C; and A, B and C are given constants (Antoine's law for water liquid-vapour equilibrium).

$$v = \frac{V_{Total}}{m_{Total}} = \frac{V_g + V_l}{m_g + m_l} = x_g \cdot v_g + x_l \cdot v_l \quad (2)$$

where v, v_g and v_l are the specific volume of the mix, the vapour and the liquid, respectively in (m^3/kg); V_g and V_l are the volume of the vapour and the liquid respectively in m^3; m_g and m_l are the weight of the vapour and the liquid respectively in kg; and finally, x_g is the vapour mass fraction and x_l the liquid mass fraction.

An external UF30 oven (Memmert, Germany) managed the temperature of the 0.1 L-non stirred reactor. The temperature in each experiment was not constant during the entire process, with a heating rate of approximately 3.5 °C min^{-1} until achieving the set temperature. Whereas the 1 L-stirred reactor allowed extracting liquid at different times, in this case, only the remaining liquid from the reaction chamber was collected and filtrated after the 2 h treatment, once the reactor stainless shell was under a safe handling temperature. It was then analysed for bromine content by ion chromatography.

The DE was defined as the fraction of bromine content removed from the solid and transferred to the liquid phase (at time 't' if applicable [in hours]), calculated using the following equation (3):

$$DE_t(\%) = \frac{m_{Br,\ Liq,t}}{m_{Br,i}} \cdot 100 \quad (3)$$

where $m_{Br,i}$ is the initial weight of bromine content in the WCB inside the reactor and $m_{Br,liq,t}$ is the weight of bromine (both in mg) in the residual liquid obtained (at time 't') from a process with no liquid extractions. The bromine content in the gas phase was not taken into account for DE calculation. According to the literature with similar WCBs, more than 99 % of bromine is emitted in the form of inorganic bromine, mainly HBr. Water has high solubility for HBr and then this compound dissolved in aqueous medium as bromide ions in the reaction conditions, in the same way as studied for HCl (Yu et al., 2016).

2.4. Analysis and characterisation of the solid residues

The solid residues obtained were separated by filtration and dried at 105 °C. Elemental analysis, Net Calorific Value (NCV) analysis, Fourier-Transform Infrared Spectroscopy (FTIR), X-ray Powder Diffraction (XRD), Thermo-Gravimetric analysis (TGA) and Differential Thermal Analysis (DTG) of the debrominated residues were also determined afterwards. The bromine content in the solid phase was analysed by ion chromatography in a previous work (Soler et al., 2017). After comparison with the bromine content in water collected from the reaction chamber, a closed bromine balance with deviation below 8 % was found. This corroborates that the majority of the Br content is transferred to aqueous phase.

2.4.1. Fourier-Transform Infrared Spectroscopy (FTIR) and X-ray Powder Diffraction (XRD)

Debrominated solid residues obtained after HTD treatment were characterised using different techniques in order to identify excess additive found in the form of solid precipitate accompanying the solid WCB residue. FTIR was conducted using BRUKER IFS 66/S (BRUKER, Germany) applying the Attenuated total reflection (ATR) method from 500 cm^{-1} to 4000 cm^{-1}. XRD was performed using BRUKER D8-ADVANCE (BRUKER, Germany) with CuKα radiation at 40 kV and a step size of 0.05° 2θ at 3 s/step in the range of 2θ from 20° to 60°.

2.4.2. Scanning electron microscopy (SEM)

The study of morphological properties of the original WCB and the

solid residues was performed by SEM using a S3000N model (Hitachi, Japan). In this way, a more specific understanding of the reaction mechanisms could be uncovered depending on the conditions used in the debromination process.

2.4.3. Thermogravimetric analysis (TGA) and Differential Thermal Analysis (DTA)

A thermogravimetric analyser Mettler Toledo TGA/SDTA851e/SF/1100 was used to investigate the decomposition behaviour of the original WCB and debrominated wastes. Runs were carried out with 7 mg of sample under combustion and pyrolysis conditions at a flow rate of 100 mL min^{-1}. Heating rates of 5, 10 and 20 °C min^{-1} were used up to 850 °C, in order to avoid the fusion of fibreglass and the disabling of pots.

In order to better discern small changes that are hardly observable in thermogravimetric (TG) curves, the TG data were also represented using derivative thermogravimetric (DTG) curves. The technique proposed by Caballero and Conesa (2005) was used to filter data and minimise background noise.

3. Results and discussion

3.1. Debromination of WCBs and optimal HTD parameters using K_2CO_3

Fig. 1 shows the evolution of the DE obtained at different time values during the runs performed at 225, 250 and 275 °C for the 1 L-stirred reactor. As can be observed, there was a notable increase of DE with temperature and a clear leap between 250 °C and 275 °C. The thermal degradation of WCB started to take place in this temperature interval (shown later in Fig. 10A and B). Results for runs at 225 °C and 250 °C were similar despite the temperature gap. However, for runs at 225 °C the WCB was cut into smaller pieces in order to observe the effect of the particle size. As a result, this difference in particle sizing compensated the temperature decrease of 25 °C, which proved the importance of the particle size. Therefore, by decreasing the particle size at a given temperature, DE could be improved for each residence time, or residence time could be reduced to achieve a specific DE.

In this way, an HTD process with agitation should be useful to reduce residence times, where no optimal conditions are followed (low additive concentration, high S/L ratios, …), in order to achieve a complete debromination and a solid residue that could be useful for fuel purposes due to their NCV after a relevant exhaust gases analysis that ensures the good quality in terms of emissions suggested by previous results of our group. In fact, lower levels of toxic emissions such as polycyclic aromatic hydrocarbons and brominated phenols compared to the initial samples were observed in one of our previous works (Soler et al., 2017). No data are available from combustion after debromination, but the levels of brominated phenols, dioxins and furans found by Ortuño et al. (2014) from combustion of the initial material are expected to be reduced with previous debromination.

Fig. 2 reveals the effect of the temperature for the 1 L-stirred reactor experiments. It can be observed that despite the treatment temperature and achieved DE, the weight loss due to the elimination of bromine and to the degradation of the resin constituent of the WCB is kept low and the resin weight lost by thermal degradation is almost unchanged. Global mass balances of the process were carried out, finding only differences below 5 % when comparing liquid plus solid mass between initial and final states. These differences are of the order of the experimental error. The amount of gas generated was therefore very small.

Fig. 3 shows some results of the runs performed at the lowest temperature (200 °C). A clear improvement of the DE yields can be observed as the S/L ratio decreases. This means that a higher amount of liquid (water) for a specific amount of solid decreases the DE. In view of these results, no further experiments with S/L ratio 1:10 or higher were necessary.

Fig. 3 also shows the evolution of DE with CO_3^{2-}/Br^- ratios. DE increases when CO_3^{2-}/Br^- ratio increases.

Fig. 4 shows the results from the runs performed at 225 °C in the 0.1 L-non stirred vessel. The observed effect is similar to that found at 200 °C (Fig. 3), but at the higher temperature of 225 °C for a S/L ratio of 1:2, a limit close to a DE of 100% is achieved as the CO_3^{2-}/Br^- ratio continues to increase.

Considering the runs performed at a CO_3^{2-}/Br^- ratio of 1:1, the maximum accomplishable DE is 92.3%, and increasing the amount of additive (CO_3^{2-}/Br^- ratios of 2:1 and 4:1) did not introduce any improvement. Therefore, even without any stirring during the HTD treatment, the optimum parameters to maximise the debromination efficiency of WCB are a solid/liquid ratio of 1:2 and a CO_3^{2-}/Br^- ratio of 1:1, where either the treatment temperature or the residence time could be slightly increased to achieve full 100 % DE. Under these reaction conditions, unreacted K_2CO_3 begins to precipitate during cooling (once the debromination treatment has ended) and weight loss is therefore distorted. In fact, the last runs performed show that there is no weight loss in the solid residue after the debromination reactions conducted

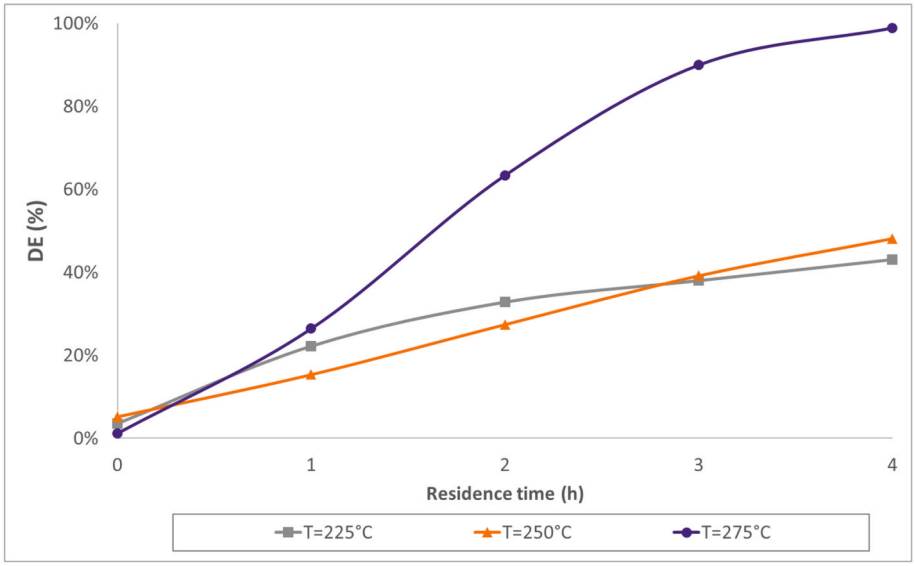

Fig. 1. DE obtained with CO_3^{2-}/Br^- ratio 1:25 and solid/liquid ratio 1:5 for several temperatures and residence times (1 L-stirred reactor).

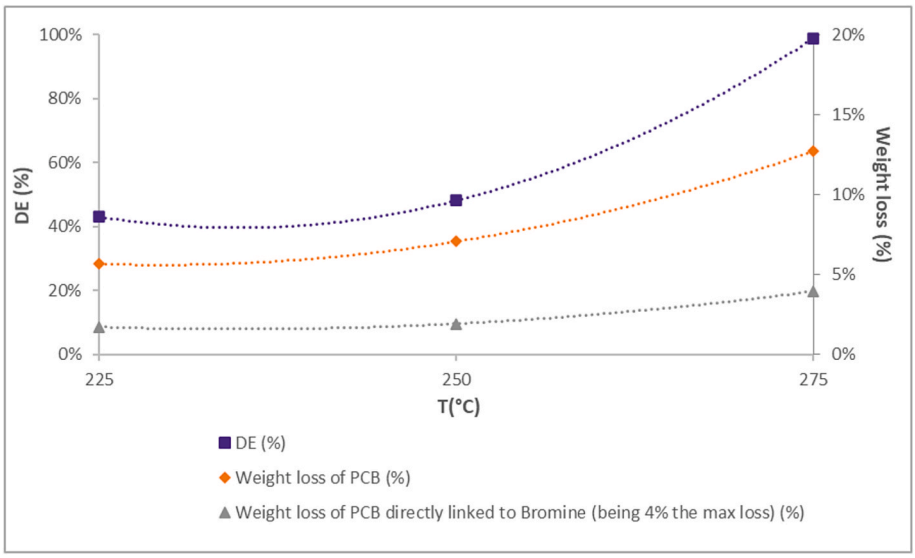

Fig. 2. Anionic ratio 1:25 and S/L 1:5 (1 L-stirred reactor) with a graph visual presentation set to read DE from the left side axis and weight losses from the right-side axis.

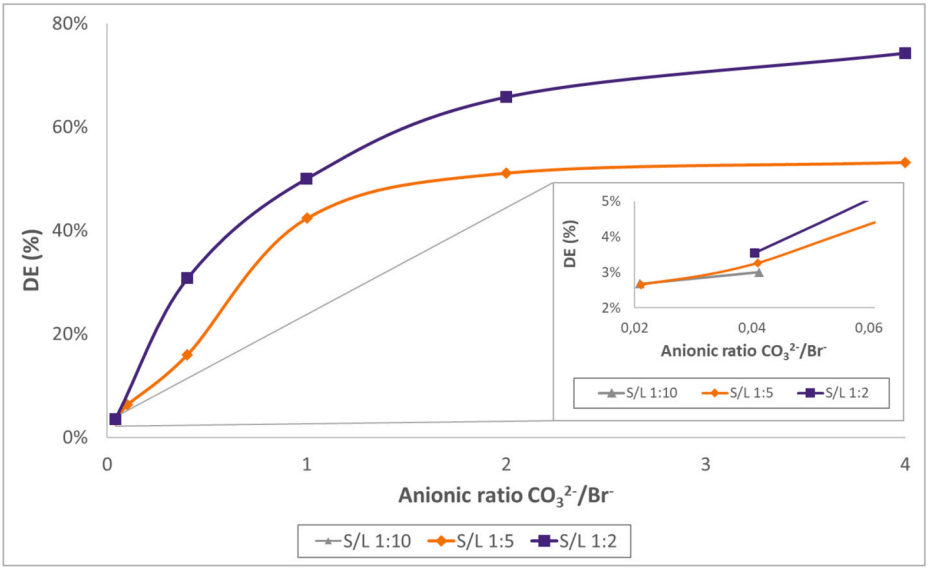

Fig. 3. DE of WCB obtained at 200 °C for several CO_3^{2-}/Br^- ratio and solid/liquid ratios (0.1 L-non stirred reactor).

from a given anionic CO_3^{2-}/Br^- ratio onwards, even after reaching a DE of 100 % as shown in Fig. 5. This could be due to the excess of additive used to accelerate the reaction, that finally precipitates as a solid at the end of the reaction. In order to complement this hypothesis, some solid residue obtained under such reaction conditions were chosen and analysed by FTIR and XRD, in addition to the SEM analysis.

In parallel, both reactors were subjected to similar reaction conditions (225 °C, solid/liquid ratio of 1:5, CO_3^{2-}/Br^- ratio of 1:25, residence time of 2 h and the same smallest WCB feeding size), the only major difference being the stirring. A DE of 32.8 % and 11.8 % were reached with and without stirring, respectively. In this way, stirring can improve DE and it could be used if necessary, even though raising the level of required maintenance, to counteract the effect of WCB feed particle sizing. Nevertheless, a reactor without stirring is the simplest option for a possible industrialization. For this reason, optimizing conditions in a non-stirred reactor was worthwhile and would certainly be the best way to debrominate WCB when optimal conditions that allow to reduce residence time and temperature of treatment for a complete debromination are followed. There are several advantages of non-stirred vs stirred treatment conditions that furnish better starting points for a future industrialization of the process: lesser energy input needed, a low price and high availability of potassium carbonate, lower equipment and operational costs, durable and easy to maintain attributes of a standard and a more affordable non-stirred high-pressure reactor with lower maintenance costs, lower equipment complexity, higher treatment capacity and particle size treatment capacity (no stirrer inside), increased cleanability of equipment, plus the possibility of improving its viability in the future through the potential reuse of unbroken WCB fibreglass. Although waste liquid left needs detailed research done aside from further investigation, in a previous similar research using chlorine instead of bromine, phenol, benzoic acid, benzaldehyde, cyclohexanone and methyl cyclopentane were identified in the liquid phase, with a low total concentration (Takeshita et al., 2004).

Moreover, Fig. 6 shows a linear correlation between the DE achieved and the weight loss of WCB (DE = 8.6689x - 0.1112 with $R^2 = 0.9941$), found after including all launched experiments except those with a

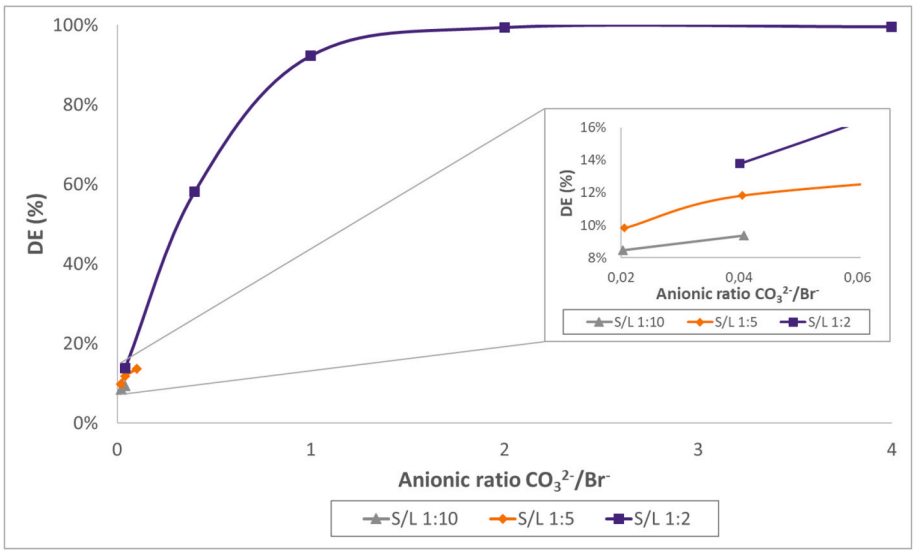

Fig. 4. DE of WCB obtained at 225 °C for several CO_3^{2-}/Br^- ratio and solid/liquid ratios (0.1 L-non stirred reactor).

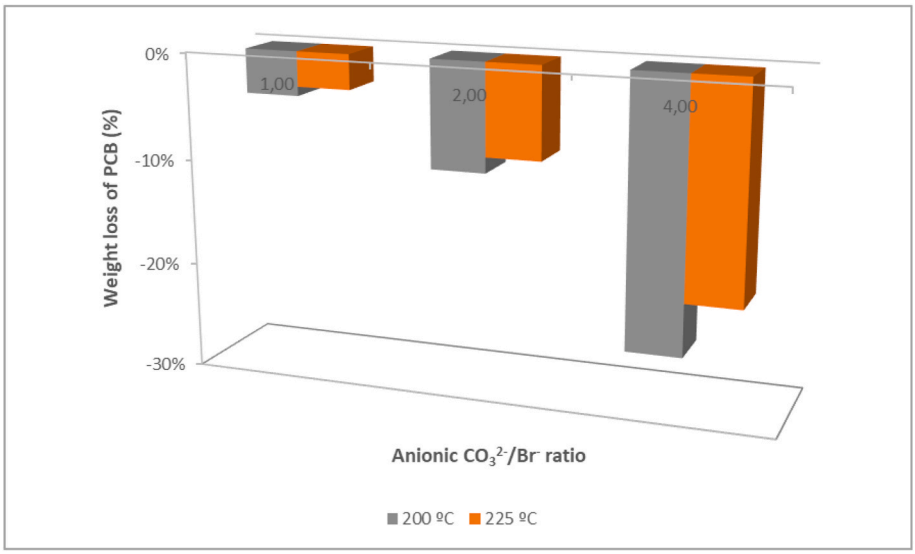

Fig. 5. Excess of additive with anionic ratio above 1:1 at S/L ratio 1:2.

CO_3^{2-}/Br^- ratio and S/L ratio above 1:5.

3.2. Characteristics of the HTD solid residues

Table 2 presents the elemental composition and Net Calorific Value (NCV) of solid residues obtained after debromination of the two series of runs, where only temperature (R225-275 °C_s/l 1:5_r 1:25) or anionic ratio (R225 °C_s/l 1:2_r 1:25–4:1) are changed. The NCV of those residues are close to those of wheat straw and agricultural waste such as sawdust (12500 kJ/kg and 13400 kJ/kg, respectively).

All residues obtained after debromination present a very similar NCV around 10500 kJ/kg, with slight variations of around 5 %. The replicates done for several samples showed a standard deviation of 3 %. In this way, it can be affirmed that the NCV remains almost constant after the HTD process.

It can be observed that the O/C ratio (Fig. 7A) and the percentage of O (wt. %) (Fig. 7B and C) strongly increase in both series of experiments. This could be explained by the fact that as the debromination treatment progresses, a high fraction of SiO_2 fibreglass is obtained at the end.

In this way, H (wt. %), C (wt. %) and N (wt. %) decrease in comparable proportions. The H/C ratio is almost maintained across both series of experiments which could explain, in addition to what is observed in Fig. 2, the small decrease in NCV after HTD treatment.

In fact, these results may anticipate the fact that the solid debrominated products obtained via both routes (varying temperature, or CO_3^{2-}/Br^- ratio) would apparently be analogous.

In Fig. 8A, the main diffraction peaks corresponding to K_2CO_3 could be found in each XRD pattern of the analysed solid residues, coming from experiments randomly chosen as a representation of the set of cases in excess of additive conditions (R200.19, R200.20 and R225.9). As those XRD samples were prepared in order to detect the precipitated from a high fibre percentage residue and manually selected, only affirming the presence or not of a representative peak (in a qualitative way) would be reasonably correct during Fig. 8A and Fig. 8B discussions.

By ATR-FTIR analysis (Fig. 8B), typical free CO_3^{2-} ion vibrations that properly represent K_2CO_3 with a vibration around 1750 cm^{-1}, 1400 cm^{-1} and 1060 cm^{-1} (Rojac et al., 2009) are denoted and found on the FTIR spectra of the 3 different solid residues. In this case, raw materials that were employed during experimentation were analysed too. It can be

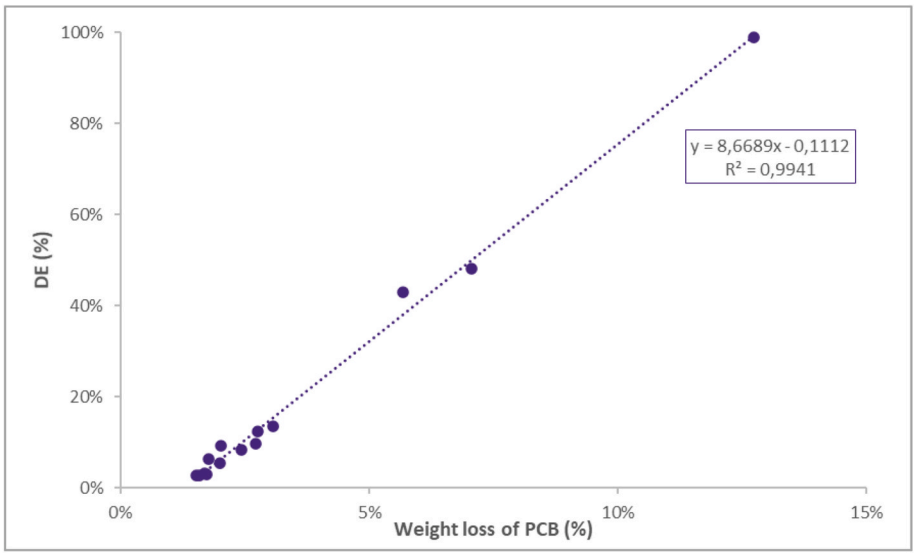

Fig. 6. Experiments for Anionic ratio and S/L ratio under 1:5 (including both reactors).

Table 2
Van Krevelen diagram represented series of experiments.

	Time (h)	Experiment residue[a]	C (wt. %)	H (wt. %)	N (wt. %)	O (wt. %)	Ash (wt. %)	H/C	O/C	NCV[b] (kJ/kg)
		Original PCB	27.55	2.54	1.06	24.56	44.29	1.11	0.67	10854
R225–275 °C_s/l 1:5_ r 1:25	4	R225.0	26.04	2.40	0.81	26.96	43.78	1.11	0.78	11239
		R250.0	23.17	2.08	0.64	32.71	41.40	1.08	1.06	11134
		R275.0	22.96	2.14	0.71	33.55	40.64	1.12	1.10	10292
R225 °C_ s/l 1:2_ r 1:25–4:1	2	R225.6	27.85	2.62	1.01	23.91	44.61	1.13	0.64	10927
		R225.7	27.49	2.56	0.83	26.52	42.60	1.12	0.72	10965
		R225.8	26.48	2.36	0.79	29.14	41.23	1.07	0.83	10784
		R225.9	26.38	2.46	0.82	30.74	39.60	1.12	0.87	10608
		R225.10	22.20	2.10	0.56	35.45	39.68	1.14	1.20	10444

[a] S (wt. %) n.d.
[b] NCV-Net calorific value.

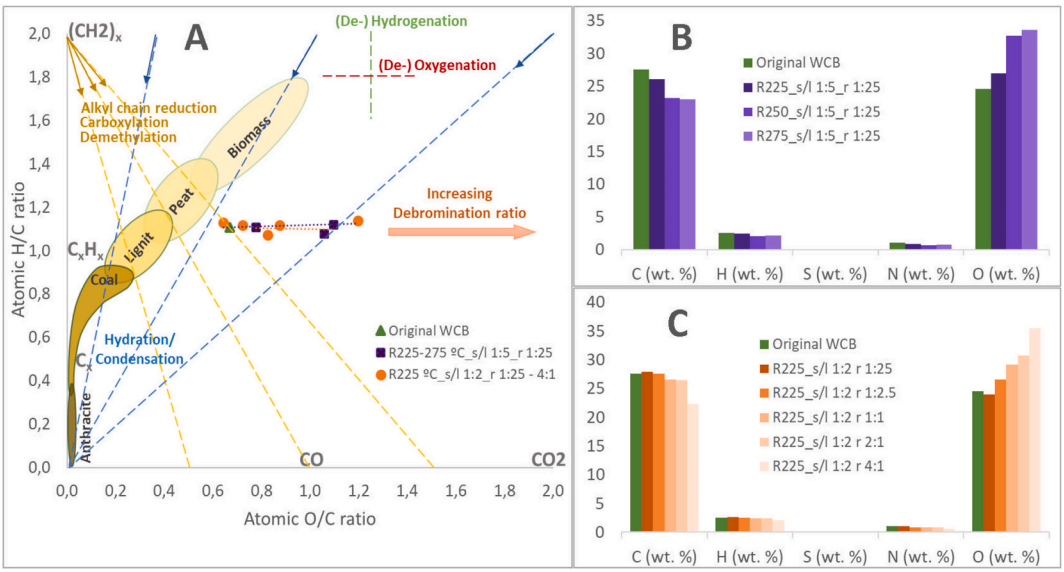

Fig. 7. A.Van Krevelen diagram where two series of runs are shown in addition to the original WCB that appears as a single green triangle: a series in purple squares (R225-275 °C_s/l 1:5_r 1:25) corresponding to 1 L-stirred reactor experiments, and a series in orange circles (R225 °C_s/l 1:2_r 1:25–4:1) corresponding to 0.1 L-non-stirred reactor runs. In this Van Krevelen diagram, blue lines describe hydration/condensation routes and arrows point in the direction of loss of H_2O. Yellow lines and arrows describe routes and ways to alkyl chain reduction, carboxylation and demethylation. Oxidation/reduction routes are represented by green/red lines. Fig. 7B: Elemental analysis of the solid residues corresponding to 1 L-stirred reactor experiments represented in the Van Krevelen diagram. Fig. 7C: Elemental analysis of the solid residues corresponding to 0.1 L-non-stirred reactor experiments represented in the Van Krevelen diagram.

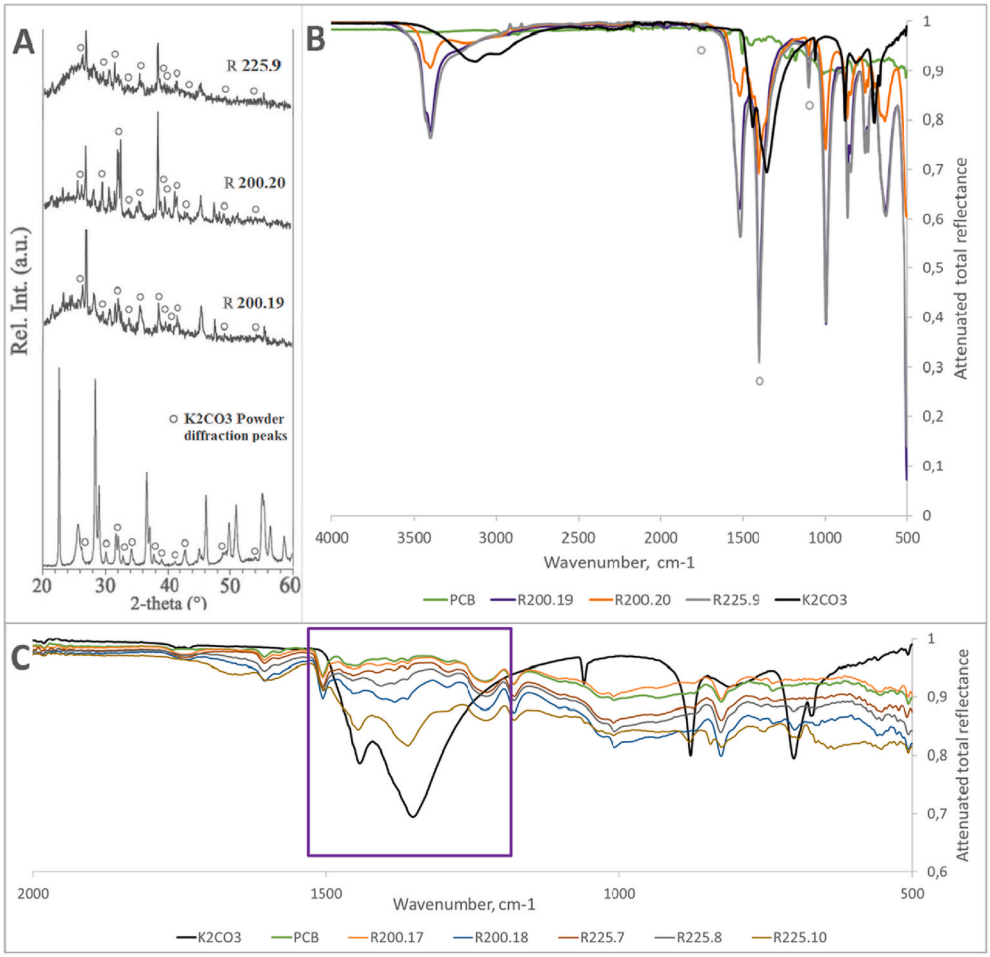

Fig. 8. A. XRD spectra of a non-milled K_2CO_3 mixture (K2CO3, Powder diffraction file 71–1466 (PDF-2 database), n.d.) at the bottom (diffraction peaks are identified with little black circles) and after the debromination process in the 0.1 L-non stirred reactor with a CO_3^{2-}/Br^- ratio of 2:1 and 4:1 at 200 °C and a CO_3^{2-}/Br^- ratio of 2:1 at 225 °C, corresponding to 3 aleatory residues of experiments in excess of additive conditions where portions of sample with visible additive precipitate were manually selected (see Table S1). Fig. 8B. FTIR patterns of the solid residues (same 3 experiments where portions of sample with visible additive precipitate were manually selected) with circles denoting CO_3^{2-} vibrations. Fig. 8C. FTIR patterns of the other solid residues (R200.17, R200.18, R225.7, R225.8 and R225.10 with anionic ratios between 1:2.5 and 4:1 where sample were accordingly homogenized via cryogenic milling).

observed that PCBs spectra were completely different to the rest, because portions of the 3 aleatory residues samples where only visible additive precipitate was really present were manually selected from the heterogenous samples with a high fibre percentage. Additionally, those other spectra seem to be similar (or identical in the case of our K_2CO_3 spectrum) to the ATR-FTIR mid-range spectrum of pure K_2CO_3 (Vahur et al., 2016). There is a lag between K_2CO_3 spectrum and residues spectra maybe because their analysis was launched in two batches with several months apart for Covid19 reasons and FTIR equipment setting could be slightly different. Since the results of both methods match, the precipitation appearing on solid residues coming from an excess of additive condition could be confirmed as K_2CO_3 and no further analysis was required.

Once the precipitate was identified as K_2CO_3, and so as to confirm by FTIR analysis the optimum anionic ratio of 1:1 commented before during Fig. 4 discussion, several solid residues with anionic ratios between 1:2.5 and 4:1 (around this optimal 1:1), accordingly homogenized by cryogenic milling, were analysed. In Fig. 8C, it can be observed that now the spectra of the solid residues were more similar to the spectrum of original PCB, confirming that PCB was not degraded in excess during debromination process. Due to homogenisation milling, K_2CO_3 precipitated was diluted inside the solid residue and not detectable by FTIR except in its largest CO_3^{2-} ion vibrations around 1400 cm^{-1} (purple frame in Fig. 8C). Regardless of the temperature carried out during debromination treatment, this peak decreased as the ratio was decreasing (starting from a maximum peak corresponding to R225.10 with an anionic ratio of 4:1), ending up with a spectrum similar to PCBs spectra for R200.17 and R225.7 (solid residues with an anionic ratio of 1: 2.5). For R200.18 and R225.8 (an anionic ratio of 1: 1), a minimum peak was observed. Together with the great DE achieved of 92.3 % as was commented before during Fig. 4 discussion, this only confirms that the optimum was very close to 1:1.

Fig. 9A and B, which corresponds to a crushed original WCB sample and an incomplete debromination sample respectively, offers a glimpse of the laminated structural design in layers with 90° intertwined fibreglass. It can be observed how, for an incomplete debromination sample under a DE of 30 % (Fig. 9B), only the most superficial resin could be degraded by the HTD process leaving some slight grooves between the fibres.

The main difference between the solid residues recovered in the 1 L-stirred reactor (Fig. 9C) and in the 0.1 L-non stirred reactor (Fig. 9D) was related to the stirring. However, fibres appear clean on both images which confirms that a complete debromination could be achieved. In this way, the advantage of the non-stirring reactor was the recovery of tidy fibres. This could be employed further on to investigate the recovery of fibres from WCB.

The disadvantage of using an excess of additive above a CO_3^{2-}/Br^- ratio of 1:1 (Fig. 9D) is that the fibre becomes surrounded by additive precipitates (Fig. 9E) and completely covered by a precipitated additive in the form of sequins (Fig. 9F), leading to the need to pre-wash before reuse where necessary, as well as the pointless use of more additive than necessary.

Therefore, along with the great DE achieved of 92.3 % as was commented before during Fig. 4 discussion and the discussion of Fig. 8C respecting FTIR results, SEM analysis results observed on Fig. 9D should be enough to appreciate that the optimum dosage correspond to an anionic ratio 1:1.

Fig. 10 presents the thermal decomposition curves obtained. In the

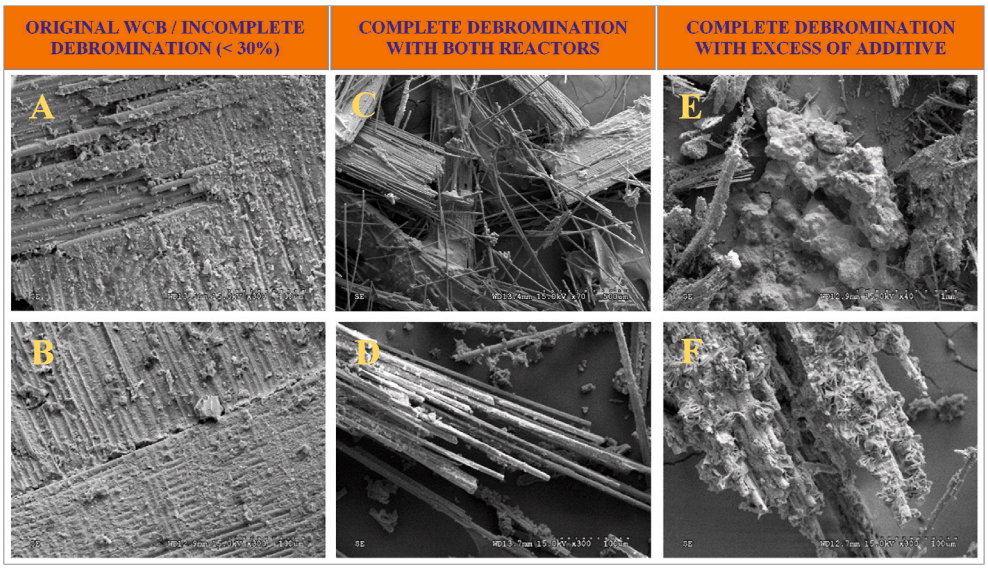

Fig. 9. SEM images of several WCB materials (A = Original crushed WCB, B = After an incomplete debromination under 30 %, C= Complete debromination achieved in a 1 L-stirred reactor, D = Complete debromination achieved in a 0.1 L-non stirred reactor, E = Precipitated additive, F = Complete debrominated WCB fibreglass wrapped up in precipitated additive).

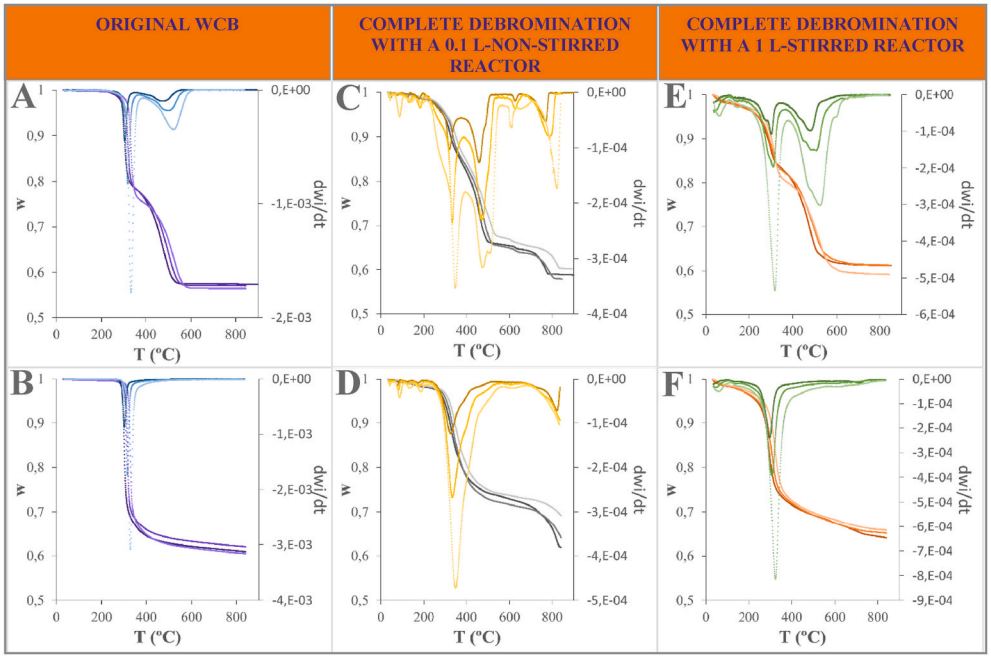

Fig. 10. Thermal decomposition of several WCB materials (A, B = TGs appear in purple and DTGs appear in blue; C, D = TGs appear grey and DTGs appear yellow; E, F = TGs appear in orange and DTGs appear in green) after debromination in air (combustion runs A, C and E) and N_2 (pyrolysis runs B, D and F) at 5, 10 and 20 °C min^{-1}. In the graphs w is defined as the mass fraction of solid, i.e., it represents the relationship between the total mass of solid at any moment (m) with respect to the initial solid mass (m_0).

presence of oxygen, two different mass loss processes are clearly observed for the original WCB and the solid residue coming from a complete debromination HTD process with the 1 L-stirred reactor (DTGs help to better visualise those changes). In pyrolysis conditions, only one process of mass loss is observed for the same two samples. However, in Fig. 10C and D, where the solid residue is coming from a complete debromination HTD process with the 0.1 L-non stirred reactor (with excess of additive), an additional process of mass loss appears at a temperature under 700 °C for both atmosphere conditions. This latter mass loss is due to the precipitate of potassium carbonate that also starts to degrade (Aracil, 2008).

As shown in Fig. 11, the total mass loss of debrominated WCB decreases with the increase of DE. It seems, however, to be more pronounced for R225.9 in both conditions. This could reveal the use of the anionic CO_3^{2-}/Br^- ratio (and definitely the use of K_2CO_3) as a parameter that could influence WCB debromination even more than temperature, once a minimum appropriate temperature is reached to enable the activation reaction.

4. Conclusions

Considering the results obtained, the stirred reactor allows complete debromination of WCB with a larger particle size even at very low anionic ratios (small amount of additive) but at slightly higher temperatures (275 instead of 225 °C) for these conditions.

On the other hand, the non-stirred one requires a lower particle size and higher anionic ratio (although the additive cost is low) to obtain similar results due to its temperatures and pressure limitations.

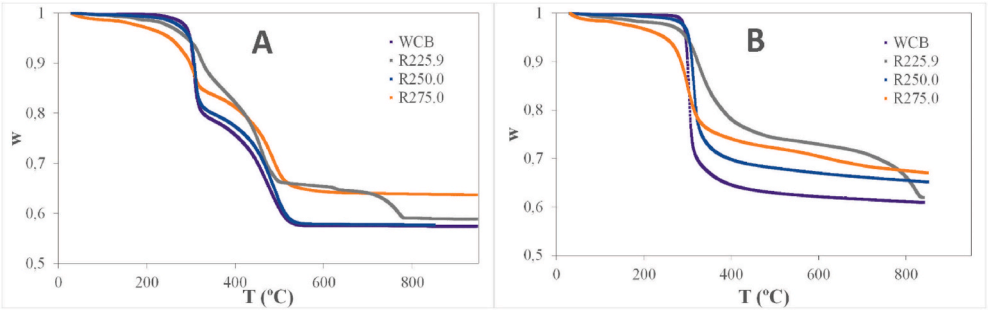

Fig. 11. Thermal decomposition of original WCB and several solid residues after debromination in air (A) and N_2 (B) at 5 °C min^{-1}. The solid residues visualised are the same as in Fig. 10 and R250.0 corresponds to an incomplete debromination. In the graphs w is defined as the mass fraction of solid, i.e., it represents the relationship between the total mass of solid at any moment (m) with respect to the initial solid mass (m_0).

However, by increasing and optimizing anionic ratio and solid-liquid ratio employed and thus favouring the reaction conditions, this achieves complete debromination at a lower temperature and less time (approximately in half the time). In addition, the industrialization process is simplified with the non-stirred reactor due to its lower complexity, lower maintenance and additional cost, and a much higher load capacity since there is no stirrer taking up space inside the reactor. This could also allow feeding the reactor with a particle size as large as the volume of the reactor, allowing to simplify the process even more (although this would lower the DE). The results of this last hypothesis may be revealed in a forthcoming study to be published. A simple scheme of the proposed batch process is shown in Figure A1 of the Appendix.

In Table A1 of the appendix, a tabular comparison between this work and main existing literature data of the last decade was done (according to our knowledge), respecting experimental conditions assessed during similar complete debromination treatments (in non-stirred reactors) of flame retardants present on PCBs with similar sizing and using water as solvent (best green and sustainable solvent). It can be observed how the temperature of treatment process (the main controlling parameter of HTD process) has been able to decrease over time in this decade from 400 °C until being almost halved in this work to 225 °C, becoming now a temperature easily achievable by any standard equipment. Additionally, anionic ratio remains in the average of what has been used so far (employing low cost and high availability additives) and solid/liquid ratio has been reduced, thus allowing to limit the amount of water used up to 8 times less. By the way, the pressure inside the reactor (vapour pressure of the mix taking into account the temperature value) has been reduced up to 8 times less too, allowing the use of reactors much simpler from a technical and mechanical point of view. In return, residence time has been increased by 1 h in order to achieve these improvements.

Therefore, these conditions improve feasibility and strengthen future industrialization of this waste management process, although it may be interesting to consider a detailed Life Cycle Analysis (LCA) further on a future work.

CRediT authorship contribution statement

Gerard Gandon-Ros: Conceptualization, Methodology, Software, Validation, Formal analysis, Investigation, Resources, Data curation, Writing – original draft, Writing – review & editing, Visualization, Project administration. **Aurora Soler:** Methodology, Resources, Writing – original draft. **Ignacio Aracil:** Conceptualization, Methodology, Writing – review & editing, Supervision. **María Francisca Gómez-Rico:** Validation, Writing – review & editing, Visualization. **Juan A. Conesa:** Conceptualization, Methodology, Writing – review & editing, Funding acquisition.

Declaration of competing interest

The authors declare that they have no known competing financial interests or personal relationships that could have appeared to influence the work reported in this paper.

Acknowledgements

Support for this work was granted by CTQ2016-76608-R project and the scholarship BES-2017-080382 from the Ministry of Economy, Industry and Competitiveness (Spain).

Appendix A. Supplementary data

Supplementary data to this article can be found online at https://doi.org/10.1016/j.jclepro.2021.128605.

APPENDIX

Supporting information is provided with 1 table and 1 figure related to this article.

References

Akcil, A., Erust, C., Gahan, C.S., Ozgun, M., Sahin, M., Tuncuk, A., 2015. Precious metal recovery from waste printed circuit boards using cyanide and non-cyanide lixiviants – a review. Waste Manag. 45, 258–271. https://doi.org/10.1016/j.wasman.2015.01.017.

Altarawneh, M., Dlugogorski, B.Z., 2015. Formation of polybrominated dibenzofurans from polybrominated biphenyls. Chemosphere 119, 1048–1053. https://doi.org/10.1016/j.chemosphere.2014.09.010.

Baldé, C.P., Forti, V., Gray, V., Kuehr, R., Stegmann, P., 2017. The Global E-Waste Monitor – 2017. United Nations University (UNU), International Telecommunication Union (ITU) & International Solid Waste Association (ISWA), Bonn/Geneva/Vienna.

Buekens, A., Yang, J., 2014. Recycling of WEEE plastics: a review. J. Mater. Cycles Waste Manag. 16, 415–434. https://doi.org/10.1007/s10163-014-0241-2.

Caballero, J.A., Conesa, J.A., 2005. Mathematical considerations for nonisothermal kinetics in thermal decomposition. J. Anal. Appl. Pyrolysis 73, 85–100. https://doi.org/10.1016/j.jaap.2004.12.003.

Chien, Y.-C., Paul Wang, H., Lin, K.-S., Huang, Y.-J.J., Yang, Y.W., 2000. Fate of bromine in pyrolysis of printed circuit board wastes. Chemosphere 40, 383–387. https://doi.org/10.1016/s0045-6535(99)00251-9.

Das, A., Vidyadhar, A., Mehrotra, S.P., 2009. A novel flowsheet for the recovery of metal values from waste printed circuit boards. Resour. Conserv. Recycl. 53, 464–469. https://doi.org/10.1016/j.resconrec.2009.03.008.

ECS, 2010. Solid Biofuels - Determination of Ash Content.

European Commission, Comisión Europea, 2012. Directiva 2012/19/UE del Parlamento Europeo y del Consejo de 4 de julio de 2012 sobre residuos de aparatos eléctricos y electrónicos (RAEE).

Gandon-Ros, G., Soler, A., Aracil, I., Gómez-Rico, M.F., 2020. Dechlorination of polyvinyl chloride electric wires by hydrothermal treatment using K2CO3 in subcritical water. Waste Manag. 102, 204–211. https://doi.org/10.1016/j.wasman.2019.10.050.

Goosey, M., Kellner, R., 2003. Recycling technologies for the treatment of end of life printed circuit boards (PCBs). Circ. World 29, 33–37. https://doi.org/10.1108/03056120310460801.

Goosey, M., Kellner, R., 2002. A Scoping Study: End-Of-Life Printed Circuit Boards. Department of Trade and Industry, Intellect & Shipley Europe Limited, London.

Guo, J., Jiang, Y., Hu, X., Xu, Z., 2012. Volatile organic compounds and metal leaching from composite products made from fiberglass-resin portion of printed circuit board waste. Environ. Sci. Technol. 46, 1028–1034. https://doi.org/10.1021/es2029558.

Guo, J.J., Guo, J.J., Xu, Z., 2009. Recycling of non-metallic fractions from waste printed circuit boards: a review. J. Hazard Mater. 168, 567–590. https://doi.org/10.1016/j.jhazmat.2009.02.104.

Hadi, P., Ning, C., Ouyang, W., Xu, M., Lin, C.S.K.K., McKay, G., 2015. Toward environmentally-benign utilization of nonmetallic fraction of waste printed circuit boards as modifier and precursor. Waste Manag. 35, 236–246. https://doi.org/10.1016/j.wasman.2014.09.020.

Ignacio Aracil Sáez, 2008. Formacion de contaminantes y estudio cinetico de la pirolisis y combustion de plasticos PE, PVC y PCP, vol. 414. Univ. Alicant.

K2CO3, Powder Diffraction File 71-1466 (PDF-2 database), n.d.

Kim, Y.-M.M., Han, T.U., Watanabe, C., Teramae, N., Park, Y.-K.K., Kim, S., Hwang, B., 2015. Analytical pyrolysis of waste paper laminated phenolic-printed circuit board (PLP-PCB). J. Anal. Appl. Pyrolysis 115, 87–95. https://doi.org/10.1016/j.jaap.2015.06.013.

Leung, A.O.W., Duzgoren-Aydin, N.S., Cheung, K.C., Wong, M.H., 2008. Heavy metals concentrations of surface dust from e-waste recycling and its human health implications in southeast China. Environ. Sci. Technol. 42, 2674–2680. https://doi.org/10.1021/es071873x.

Nie, Z., Liu, G., Liu, W., Zhang, B., Zheng, M., 2012. Characterization and quantification of unintentional POP emissions from primary and secondary copper metallurgical processes in China. Atmos. Environ. 57, 109–115. https://doi.org/10.1016/j.atmosenv.2012.04.048.

Ning, C., Lin, C.S.K., Hui, D.C.W., McKay, G., 2017. Waste printed circuit board (PCB) recycling techniques. Top. Curr. Chem. 375, 43. https://doi.org/10.1007/s41061-017-0118-7.

Ortuño, N., Conesa, J.A., Moltó, J., Font, R., 2014. Pollutant emissions during pyrolysis and combustion of waste printed circuit boards, before and after metal removal. Sci. Total Environ. 499, 27–35. https://doi.org/10.1016/j.scitotenv.2014.08.039.

Owens, C.V., Lambright, C., Bobseine, K., Ryan, B., Gray, L.E., Gullett, B.K., Wilson, V.S., 2007. Identification of estrogenic compounds emitted from the combustion of computer printed circuit boards in electronic waste. Environ. Sci. Technol. 41, 8506–8511. https://doi.org/10.1021/es071425p.

Pitea, D., Bortolami, M., Collina, E., Cortili, G., Franzoni, F., Lasagni, M., Piccinelli, E., 2008. Prevention of PCDD/F formation and minimization of their emission at the stack of a secondary aluminum casting plant. Environ. Sci. Technol. 42, 7476–7481. https://doi.org/10.1021/es800976s.

Rojac, T., Kosec, M., Połomska, M., Hilczer, B., Šegedin, P., Bencan, A., 2009. Mechanochemical reaction in the K2CO3-Nb2O5 system. J. Eur. Ceram. Soc. 29, 2999–3006. https://doi.org/10.1016/j.jeurceramsoc.2009.04.017.

Sakai, S., Watanabe, J., Honda, Y., Takatsuki, H., Aoki, I., Futamatsu, M., Shiozaki, K., 2001. Combustion of brominated flame retardants and behavior of its byproducts. Chemosphere 42, 519–531. https://doi.org/10.1016/s0045-6535(00)00224-1.

Soler, A., Conesa, J.A., Ortuño, N., 2017. Emissions of brominated compounds and polycyclic aromatic hydrocarbons during pyrolysis of E-waste debrominated in subcritical water. Chemosphere 186, 167–176. https://doi.org/10.1016/j.chemosphere.2017.07.146.

Takeshita, Y., Kato, K., Takahashi, K., Sato, Y., Nishi, S., 2004. Basic study on treatment of waste polyvinyl chloride plastics by hydrothermal decomposition in subcritical and supercritical regions. J. Supercrit. Fluids 31, 185–193. https://doi.org/10.1016/j.supflu.2003.10.006.

US EPA, 2000. Method 9056A. Determination of Inorganic Anions by Ion Chromatography. SW-846.

US EPA, 1994. Method 5050. Bomb Preparation Method for Solid Waste. SW-846.

Vahur, S., Teearu, A., Peets, P., Joosu, L., Leito, I., 2016. ATR-FT-IR spectral collection of conservation materials in the extended region of 4000-80 cm–1. Anal. Bioanal. Chem. 408, 3373–3379. https://doi.org/10.1007/s00216-016-9411-5.

Wang, Y., Zhang, F.-S., 2012. Degradation of brominated flame retardant in computer housing plastic by supercritical fluids. J. Hazard. Mater. 205–206, 156–163. https://doi.org/10.1016/j.jhazmat.2011.12.055.

Xing, M., Zhang, F.S., 2013. Degradation of brominated epoxy resin and metal recovery from waste printed circuit boards through batch sub/supercritical water treatments. Chem. Eng. J. 219, 131–136. https://doi.org/10.1016/j.cej.2012.12.066.

Xiu, F.R., Qi, Y., Zhang, F.S., 2014. Co-treatment of waste printed circuit boards and polyvinyl chloride by subcritical water oxidation: removal of brominated flame retardants and recovery of Cu and Pb. Chem. Eng. J. 237, 242–249. https://doi.org/10.1016/j.cej.2013.10.026.

Yin, J., Li, G., He, W., Huang, J., Xu, M., 2011. Hydrothermal decomposition of brominated epoxy resin in waste printed circuit boards. J. Anal. Appl. Pyrolysis 92, 131–136. https://doi.org/10.1016/j.jaap.2011.05.005.

Yu, J., Sun, L., Ma, C., Qiao, Y., Yao, H., 2016. Thermal degradation of PVC: a review. Waste Manag. 48, 300–314. https://doi.org/10.1016/j.wasman.2015.11.041.

Zhou, X., Guo, J., Lin, K., Huang, K., Deng, J., 2013. Leaching characteristics of heavy metals and brominated flame retardants from waste printed circuit boards. J. Hazard Mater. 246–247, 96–102. https://doi.org/10.1016/j.jhazmat.2012.11.065.